

Magnetic Susceptibility of the Quark Condensate and Polarization from Chiral Models

Marco Frasca^{1,*} and Marco Ruggieri^{2,†}

¹*via Erasmo Gattamelata, 3, 00176 Roma, Italy*

²*Yukawa Institute for Theoretical Physics, Kyoto University,
Kitashirakawa Oiwake-cho, Sakyo-ku, Kyoto 606-8502, Japan*

We compute the magnetic susceptibility of the quark condensate and the polarization of quarks at zero temperature and in a uniform magnetic background. Our theoretical framework consists of two chiral models that allow to treat self-consistently the spontaneous breaking of chiral symmetry: the linear σ -model coupled to quarks, dubbed quark-meson model, and the Nambu-Jona-Lasinio model. We also perform analytic estimates of the same quantities within the renormalized quark-meson model, both in the regimes of weak and strong fields. Our numerical results are in agreement with the recent literature; moreover, we confirm previous Lattice findings, related to the saturation of the polarization at large fields.

PACS numbers: 12.38.Aw, 12.38.Mh

Keywords: Magnetic Susceptibility of the Quark Condensate, Effective Chiral Models, QCD in Strong Magnetic Background.

I. INTRODUCTION

One of the most attractive aspects of the vacuum of Quantum Chromodynamics (QCD), the theory of strong interactions, is its non-perturbative nature. Mainly by means of Lattice QCD simulations at zero quark chemical potential [1–5] it is established that two crossovers take place in a narrow range of temperature; one for quark deconfinement, and another one for the (approximate) restoration of chiral symmetry. Besides, powerful analytic and semi-analytic techniques have been developed to understand the coupling between chiral symmetry restoration and deconfinement, see [6, 7] and references therein. Moreover, Lattice QCD and Operator Product Expansion (OPE in the following) of the correlators of hadronic currents show that the QCD vacuum can be characterized by several quark, gluon and mixed condensates [8].

A fruitful theoretical approach to the physics of strong interactions, which is capable to capture some of the non-perturbative properties of the QCD vacuum, is the use of effective chiral models. One of them is the Nambu-Jona-Lasinio (NJL) model [9] (see Refs. [10] for reviews), in which the QCD gluon-mediated interactions are replaced by effective interactions among quarks, which are built in order to respect the global symmetries of QCD. Under some approximations, it is possible to derive the NJL model effective interaction kernel from first principles QCD, see [11, 12]. Besides, a linear σ -model augmented with a Yukawa-type coupling to quarks, named Quark-Meson model (QM model in the following), has been developed as an effective model of QCD [13, 14]. In this model, quartic meson self-couplings allow to absorb the cutoff dependence of the coupling constants; moreover, following an idea by Weinberg [15], tree level prop-

agating mesons are sufficient to avoid triviality of the NJL model in $3 + 1$ dimensions in the one-loop approximation [16] (see [14] for an excellent discussion about these points).

The chiral models are widely used to map qualitatively, and to some extent also quantitatively, the phase diagram of strongly interacting matter along several directions like temperature, chemical potential, isospin chemical potential and external fields [17–30]. It is thus interesting to use these models to compute other quantities, which are related to the QCD vacuum condensates. As a matter of fact, the chiral models allow for a self-consistent treatment of the spontaneous chiral symmetry breaking in the vacuum. Therefore, after the ground state properties (i.e., the chiral condensate in the NJL model, or the expectation value of the σ -field in the quark-meson model) under external factors are computed, it is straightforward to estimate numerical values of other condensates, using the one-loop propagators of the theory.

It has been realized that external fields can induce QCD condensates that are absent otherwise [31]. Of particular interest for this article is magnetic moment, $\langle \bar{f} \Sigma^{\mu\nu} f \rangle$ where f denotes the fermion field of the flavor f -th, and $\Sigma^{\mu\nu} = -i(\gamma^\mu \gamma^\nu - \gamma^\nu \gamma^\mu)/2$. At small fields one can write, according to [31],

$$\langle \bar{f} \Sigma^{\mu\nu} f \rangle = \chi \langle \bar{f} f \rangle Q_f |eB|, \quad (1)$$

and χ is a constant independent on flavor, which is dubbed magnetic susceptibility of the quark condensate. In [31] it is proved that the role of the condensate (1) to QCD sum rules in external fields is significant, and it cannot be ignored. The quantity χ has been computed by means of special sum rules [31–35], OPE combined with Pion Dominance [36], holography [37, 38], instanton vacuum model [39], analytically from the zero mode of the Dirac operator in the background of a $SU(2)$ instanton [40], and on the Lattice in two color quenched simulations at zero and finite temperature [41]. It has also been suggested that in the photoproduction of lep-

* marcofrasca@mclink.it

† ruggieri@yukawa.kyoto-u.ac.jp

ton pairs, the interference of the Drell-Yan amplitude with the amplitude of a process where the photon couples to quarks through its chiral-odd distribution amplitude, which is normalized to the magnetic susceptibility of the QCD vacuum, is possible [42]. This interference allows in principle to access the chiral odd transversity parton distribution in the proton. Therefore, this quantity is interesting both theoretically and phenomenologically. The several estimates, that we briefly review in Section III, lead to the numerical value of χ as follows:

$$\chi \langle \bar{f} f \rangle = 40 - 70 \text{ MeV} . \quad (2)$$

A second quantity, which embeds non-linear effects at large fields, is the polarization, μ_f , defined as

$$\mu_f = \left| \frac{\Sigma_f}{\langle \bar{f} f \rangle} \right| , \quad \Sigma_f = \langle \bar{f} \Sigma^{12} f \rangle , \quad (3)$$

which has been computed on the Lattice in [41] for a wide range of magnetic fields, in the framework of two-color QCD with quenched fermions. At small fields $\mu_f = |\chi Q_f eB|$ naturally; at large fields, non-linear effects dominate and an interesting saturation of μ_f to the asymptotic value $\mu_\infty = 1$ is measured. According to [41] the behavior of the polarization as a function of eB in the whole range examined, can be described by a simple inverse tangent function. Besides, magnetization of the QCD vacuum has been computed in the strong field limit in [43] using perturbative QCD, where it is found it grows as $B \log B$.

In this article, we compute the magnetic susceptibility of the quark condensate by means of the NJL and the QM models. This study is interesting because in the chiral models, it is possible to compute self-consistently the numerical values of the condensates as a function of eB , once the parameters are fixed to reproduce some characteristic of the QCD vacuum. We firstly perform a numerical study of the problem, which is then complemented by some analytic estimate of the same quantity within the renormalized QM model. Moreover, we compute the polarization of quarks at small as well as large fields, both numerically and analytically. In agreement with the Lattice results [41], we also measure a saturation of μ_f to one at large fields, in the case of the effective models. Our results push towards the interpretation of the saturation as a non-artifact of the Lattice. On the contrary, we can offer a simple physical understanding of this behavior, in terms of lowest Landau level dominance of the chiral condensate. As a matter of fact, using the simple equations of the models for the chiral condensate and for the magnetic moment, we can show that at large magnetic field μ_f has to saturate to one, because in this limit the higher Landau levels are expelled from the chiral condensate; as a consequence, the ratio of the two approaches one asymptotically.

We also obtain a saturation of the polarization within the renormalized QM model. There are some differences, however, in comparison with the results of the non-renormalized models. In the former case, the asymptotic

value of μ_f is charge-dependent; moreover, the interpretation of the saturation as a lowest Landau level (LLL) dominance is not straightforward, because the renormalized contribution of the higher Landau levels is important in the chiral condensate, even in the limit of very strong fields. It is possible that the results obtained within the renormalized model are a little bit far from true QCD. As a matter of fact, in the renormalized model we assume that the quark self-energy is independent on momentum; thus, when we take the limit of infinite quark momentum in the gap equation, and absorb the ultraviolet divergences by means of counterterms and renormalization conditions, we implicitly assume that that quark mass at large momenta is equal to its value at zero momentum. We know that this is not true, see for example [44, 45]: even in the renormalized theory, the quark self-energy naturally cuts off the large momenta, leading to LLL dominance in the traces of quark propagator which are relevant for our study. Nevertheless, it is worth to study this problem within the renormalized QM model in its simplest version, because it helps to understand the structure of this theory under the influence of a strong magnetic field.

In our calculations we neglect, for simplicity, the possible condensation of ρ -mesons at strong fields [46, 47]. Vector meson dominance [46] and Sakai-Sugimoto model [48] suggest for the condensation a critical value of $eB_c \approx m_\rho^2 \approx 0.57 \text{ GeV}^2$, where m_ρ is the ρ -meson mass in the vacuum. Beside these, a NJL-based calculation within the lowest Landau level (LLL) approximation [47] predicts ρ -meson condensation at strong fields as well, even if in the latter case it is hard to estimate exactly eB_c , mainly because of the uncertainty of the parameters of the model. It would certainly be interesting to address this problem within our calculations, in which not only the LLL but also the higher Landau levels are considered, and in which the spontaneous breaking of chiral symmetry is kept into account self-consistently. However, this would complicate significantly the calculational setup. Therefore, for simplicity we leave this issue to a future project.

The plan of the article is as follows. In Section II we describe the QM and NJL models and fix our notation. In Section III we discuss our numerical results for the polarization of quarks, and compute the magnetic susceptibility of the quark condensate. In Section IV we compute the renormalized Quantum Effective Potential (QEP) of the QM model in a magnetic background, in the one-loop approximation, and compute analytically the solution of the gap equation in the weak field case, and semi-analytically in the strong field limit. We then use the results to estimate μ_f and χ . Finally, in Section V we draw our conclusions.

II. CHIRAL MODELS COUPLED TO A MAGNETIC FIELD

In the first part of this article, we derive numerical results for the spin polarization of quarks in a magnetic field, and for the magnetic susceptibility of the quark condensate, using two effective chiral models: the Nambu-Jona-Lasinio (NJL) model, and the Quark-Meson (QM) model. We describe the two models in some detail in this Section. We work in the Landau gauge and take the magnetic field along the z -axis, $\mathbf{B} = (0, 0, B)$.

A. Quark-Meson model

In the QM model, a meson sector described by the linear sigma model lagrangian, is coupled to quarks via a Yukawa-type interaction. The model is renormalizable in $D = 3+1$ dimensions. However, since we adopt the point of view of it as an effective description of QCD, it is not necessary to use the renormalized version of the model itself. On the contrary, it is enough to fix an ultraviolet scale to cutoff the divergent expectation values; the UV scale is then chosen phenomenologically, by requiring that the numerical value of the chiral condensate in the vacuum obtained within the model, is consistent with the results obtained from the sum rules [49]. This is a rough approximation of the QCD effective quark mass, which smoothly decays at large momenta [44, 45]. In Section IV we will use a renormalized version of the model, to derive semi-analytically some results in the two regimes of weak and strong fields.

The lagrangian density of the model is given by

$$\mathcal{L} = \bar{q} [iD_\mu \gamma^\mu - g(\sigma + i\gamma_5 \boldsymbol{\tau} \cdot \boldsymbol{\pi})] q + \frac{1}{2} (\partial_\mu \sigma)^2 + \frac{1}{2} (\partial_\mu \boldsymbol{\pi})^2 - U(\sigma, \boldsymbol{\pi}) . \quad (4)$$

In the above equation, q corresponds to a quark field in the fundamental representation of color group $SU(3)$ and flavor group $SU(2)$; the covariant derivative, $D_\mu = \partial_\mu - Q_f e A_\mu$, describes the coupling to the background magnetic field, where Q_f denotes the charge of the flavor f . Besides, σ , $\boldsymbol{\pi}$ correspond to the scalar singlet and the pseudo-scalar iso-triplet fields, respectively. The potential U describes tree-level interactions among the meson fields. In this article, we take its analytic form as

$$U(\sigma, \boldsymbol{\pi}) = \frac{\lambda}{4} (\sigma^2 + \boldsymbol{\pi}^2 - v^2)^2 - h\sigma , \quad (5)$$

where the first addendum is chiral invariant; the second one describes a soft explicit breaking of chiral symmetry, and it is thus responsible for the non-zero value of the pion mass. For $h = 0$, the interaction terms of the model are invariant under $SU(2)_V \otimes SU(2)_A \otimes U(1)_V$. This group is broken explicitly to $U(1)_V^3 \otimes U(1)_A^3 \otimes U(1)_V$ if the magnetic field is coupled to the quarks, because of the different electric charge of u and d quarks. Here, the

superscript 3 in the V and A groups denotes the transformations generated by τ_3 , $\tau_3 \gamma_5$ respectively. Therefore, the chiral group in presence of a magnetic field is $U(1)_V^3 \otimes U(1)_A^3$. This group is then explicitly broken by h -term to $U(1)_V^3$.

In this article, we restrict ourselves to the large- N_c (that is, one-loop) approximation, which amounts to consider mesons as classical fields, and integrate only over fermions in the generating functional of the theory to obtain the Quantum Effective Potential (QEP). As a matter of fact, quantum corrections arising from meson bubbles are suppressed of a factor $1/N_c$ with respect to case of the fermion bubble. In the integration process, the meson fields are fixed to their classical expectation value, $\langle \boldsymbol{\pi} \rangle = 0$ and $\langle \sigma \rangle \neq 0$ (in particular, σ has the quantum numbers of the chiral condensate, $\langle \bar{q}q \rangle$). The physical value of $\langle \sigma \rangle$ will be then determined by minimization of the QEP.

To compute QEP in presence of a magnetic background, we use the Leung-Ritus-Wang method [50] which allows to write down the quark propagator for the flavor f in terms of Landau levels,

$$S_f(x, y) = \sum_{k=0}^{\infty} \int \frac{dp_0 dp_2 dp_3}{(2\pi)^4} E_P(x) \Lambda_k \frac{i}{P \cdot \gamma - M} \bar{E}_P(y) , \quad (6)$$

where $E_P(x)$ corresponds to the eigenfunction of a charged fermion in magnetic field, and $\bar{E}_P(x) \equiv \gamma_0 (E_P(x))^\dagger \gamma_0$. In the above equation,

$$P = (p_0, 0, Q\sqrt{2k|Q_f e B|}, p_3) , \quad (7)$$

where $k = 0, 1, 2, \dots$ labels the k^{th} Landau level, and $Q \equiv \text{sign}(Q_f)$, with Q_f denoting the charge of the flavor f ; Λ_k is a projector in Dirac space which keeps into account the degeneracy of the Landau levels; it is given by

$$\Lambda_k = \delta_{k0} [\mathcal{P}_+ \delta_{Q,+1} + \mathcal{P}_- \delta_{Q,-1}] + (1 - \delta_{k0}) I , \quad (8)$$

where \mathcal{P}_\pm are spin projectors and I is the identity matrix in Dirac spinor indices. At the one-loop level, the QEP then reads

$$V = \frac{\lambda}{4} (\sigma^2 - v^2)^2 - h\sigma - N_c \sum_f \frac{|Q_f e B|}{2\pi} \sum_k \beta_k \int \frac{dp_3}{2\pi} \omega_k(p_3) . \quad (9)$$

In the above equation we have defined

$$\omega_k(p_3) = \sqrt{p_3^2 + 2k|Q_f e B| + m_q^2} , \quad (10)$$

with $m_q = g\sigma$; $\beta_k = 2 - \delta_{k0}$ counts the degeneracy of the Landau levels.

The one-loop fermion contribution, which corresponds to the last addendum in the r.h.s. of Eq. (9), is divergent in the ultraviolet. In order to regularize it, we adopt a

smooth regulator U_Λ as in [26], which is more suitable, from the numerical point of view, in our model calculation with respect to the hard-cutoff which is used in analogous calculations without magnetic field. In this article we chose

$$U_\Lambda = \frac{\Lambda^{2N}}{\Lambda^{2N} + (p_z^2 + 2|Q_f e B|k)^N}, \quad N = 5. \quad (11)$$

The (more usual) 3-momentum cutoff regularization scheme is recovered in the limit $N \rightarrow \infty$; we notice that, even if the choice $N = 5$ may seem arbitrary to some extent, it is not more arbitrary than the choice of the hard cutoff scheme, that is, of a regularization scheme. In effective models, the choice of a regularization scheme is a part of the definition of the model itself. Momentum integrals are understood as follows:

$$\sum_n \beta_n \int \frac{dp}{2\pi} \rightarrow \sum_n \beta_n \int \frac{dp}{2\pi} U_\Lambda. \quad (12)$$

Once the expectation value of σ is computed as a function of eB by a procedure of minimization of V , we compute the expectation values that are relevant to the context. To begin with, we consider the chiral condensate for the flavor f , $\langle \bar{f}f \rangle = -\text{Tr}[S_f(x, x)]$, with S_f given by Eq. (6). It is straightforward to derive the relation

$$\langle \bar{f}f \rangle = -N_c \frac{|Q_f e B|}{2\pi} \sum_{k=0}^{\infty} \beta_k \int \frac{dp_3}{2\pi} \frac{m_q}{\omega_k(p_3)}, \quad (13)$$

where the divergent integral on the r.h.s. of the above equation has to be understood regularized as in (12). From Eq. (13) we notice that the prescription (12) is almost equivalent to the introduction of a running effective quark mass,

$$m_q = g\sigma\Theta(\Lambda^2 - p_3^2 - 2k|Q_f e B|), \quad (14)$$

that can be considered as a rough approximation to the effective running quark mass in QCD [45] which decays at large quark momenta, see also the discussion in [44]. Once the scale Λ is fixed, the Landau levels with $n \geq 1$ are removed from the chiral condensate if $eB \gg \Lambda^2$.

Next we turn to the magnetic moment for the flavor f ,

$$\langle \bar{f} \Sigma^{\mu\nu} f \rangle = -\text{Tr}[\Sigma^{\mu\nu} S_f(x, x)], \quad (15)$$

where

$$\Sigma^{\mu\nu} = \frac{1}{2i}(\gamma^\mu \gamma^\nu - \gamma^\nu \gamma^\mu), \quad (16)$$

is the relativistic spin operator. We take $\mathbf{B} = (0, 0, B)$; in this case, only $\Sigma^{12} \equiv \Sigma_f$ is non-vanishing. Using the properties of γ -matrices it is easy to show that only the Lowest Landau Level (LLL) gives a non-vanishing contribution to the trace:

$$\Sigma_f = N_c \frac{Q_f |eB|}{2\pi} \int \frac{dp_3}{2\pi} \frac{m_q}{\omega_0(p_3)}, \quad (17)$$

where $\omega_0 = \omega_{k=0}$. Once again, the divergent integral on the r.h.s. of the above equation has to be understood regularized following the prescription in Eq. (12).

For the QM model, the parameters are tuned as follows. We fix the constituent quark mass in the vacuum to a phenomenological value, $m_q = 335$ MeV; furthermore, we require that in the vacuum the following condition holds:

$$\left. \frac{\partial V(\sigma, \mathbf{B} = 0)}{\partial \sigma} \right|_{\sigma=f_\pi} = 0, \quad (18)$$

which implies that $\langle \sigma \rangle = f_\pi$ in the vacuum, thus $m_q = g f_\pi$. As a consequence we find $g = 3.62$. The parameter h is fixed by the condition $h = f_\pi m_\pi^2$, where m_π is the average value of the pion mass in the vacuum and $f_\pi = 92.4$ MeV. We have then $h = 0.047 m_q^3$. To determine v and λ we solve simultaneously Eq. (18) and

$$m_\sigma^2 = \left. \frac{\partial^2 V}{\partial \sigma^2} \right|_{\sigma=f_\pi}, \quad (19)$$

with $m_\sigma = 700$ MeV. The divergences in these two equations are cured with the prescription (12). In the UV regulator we chose $\Lambda = 560$ MeV which implies $\langle \bar{u}u \rangle = (-231 \text{ MeV})^3$. This results in the values $\lambda = 4.67$ and $v^2 = -1.8 m_q^2$. Before going ahead, we notice that in the non-renormalized model, the 1-loop fermion contribution regularized at the scale Λ is included into the conditions (18) and (19).

B. Nambu-Jona-Lasinio model

The quark lagrangian density of the NJL model is given by

$$\mathcal{L} = \bar{q}(i\gamma^\mu D_\mu - m_0)q + G \left[(\bar{q}q)^2 + (i\bar{q}\gamma_5 \boldsymbol{\tau} q)^2 \right]; \quad (20)$$

here q is the quark Dirac spinor in the fundamental representation of the flavor $SU(2)$ and the color group; $\boldsymbol{\tau}$ correspond to the Pauli matrices in flavor space. A sum over color and flavor is understood. Once again, the covariant derivative embeds the QED coupling of the quarks with the external magnetic field. The explicit soft breaking of chiral symmetry in this model is achieved by introducing a current quark mass, m_0 , whose numerical value is fixed by fitting the vacuum pion mass. The NJL model is not renormalizable in the usual sense for $D > 2$ space-time dimensions; it is renormalizable in $D < 4$ in the one-loop approximation. At $D = 4$ it might represent a trivial theory of non-interacting bosons if the ultraviolet cutoff is allowed to be infinite [14, 16]. However, adopting the point of view of the NJL model as an effective (and rough) description of low-energy QCD, it is not necessary to require the cutoff to be infinite: the cutoff can be interpreted as a physical quantity which makes the effective quark mass to be constant at small quark momenta, and vanishing at large momenta, thus mimicking roughly the

running effective mass of real QCD [45]. It is worth to notice that a non-local interaction among quarks with the same quantum numbers of the four-fermion local term in Eq. (20) can be derived by the QCD action under some approximation, taking the low energy limit of the latter [7, 11]. For simplicity, we treat here only the case of local interaction.

Once again, the one-loop fermion contribution can be obtained within the Leung-Ritus-Wang method:

$$V = G\Sigma^2 - N_c \sum_{f=u,d} \frac{|Q_f eB|}{2\pi} \sum_n \beta_n \int_{-\infty}^{+\infty} \frac{dp}{2\pi} \omega_n(p), \quad (21)$$

with $\omega_n(p) = \sqrt{p^2 + 2n|Q_f eB| + M_q^2}$, and $M_q = m_0 - 2G\Sigma$ with $\Sigma = \langle \bar{u}u + \bar{d}d \rangle$. Equations (13) and (15) are still valid in the NJL model, with the replacement $m_q \rightarrow M_q$. A comparison of the QEPs of the QM model and of the NJL model shows that at the one-loop level, the two models differ only for the classic part of the effective meson potential, and for the definition of the constituent quark mass.

The parameters in the NJL model are fixed as follows. The bare quark mass is computed by virtue of the Gell-Mann-Oakes-Renner relation, $m_\pi^2 f_\pi^2 = -2m_0 \langle \bar{u}u \rangle$, which is satisfied in the NJL model [10]. Then, two equations are solved simultaneously: one for f_π and one for the chiral condensate in the vacuum at zero magnetic field strength. Requiring that $f_\pi = 92.4$ MeV and $\langle \bar{u}u \rangle = (-253 \text{ MeV})^3$, this procedure gives the numerical values of G and Λ . Thus we find $\Lambda = 626.76$ MeV, $G = 2.02/\Lambda^2$ and $m_0 = 5$ MeV.

III. NUMERICAL RESULTS

In this Section, we collect our numerical results which are relevant for the computation of the magnetic susceptibility of the chiral condensate, and of the spin polarization. From the numerical point of view, it is more convenient to compute firstly the latter; then, a fit of the polarization data at small fields will enable to extract the value of the magnetic susceptibility of the quark condensate. For what concerns data about chiral condensate, magnetic moment and polarization, we plot results only for the QM model, since the results obtained within the NJL model are qualitatively very similar to those obtained within the former model. Then, we will give the final result for the chiral magnetization for the two models considered here.

A. Polarization

The physical value of the (total) chiral condensate Σ for the NJL model, and of σ for the QM model, are obtained numerically by a minimization procedure of the QEP (21) for any value of eB . Then, we make use of

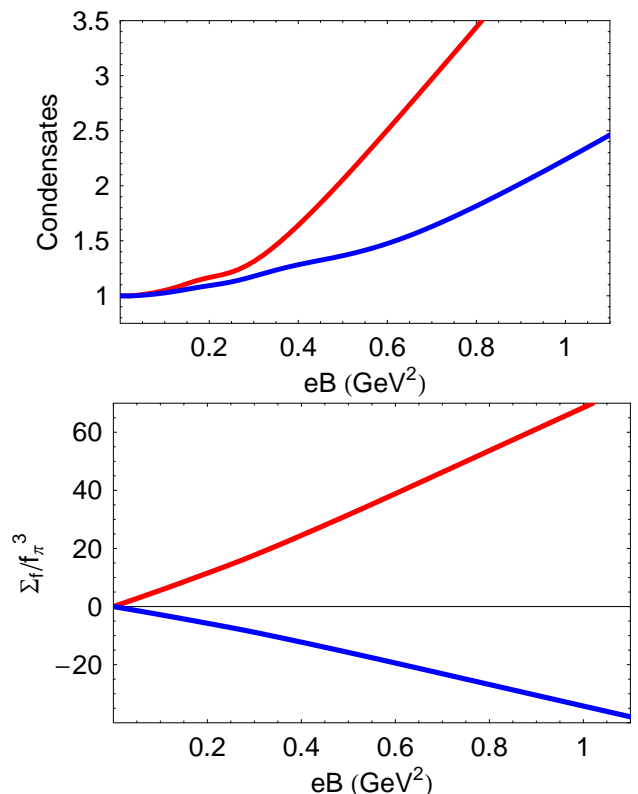


FIG. 1. *Upper panel.* Chiral condensates of u -quarks (red) and d -quarks (blue), in units of the same quantities at zero magnetic field, as a function of the magnetic field. *Lower panel.* Expectation value of the magnetic moment operator, in units of f_π^3 , as a function of eB . Data correspond to the QM model.

Eqs. (13) and (15), with the replacement (12), to compute the chiral condensate and the magnetic moment for each flavor.

In the upper panel of Fig. 1, we plot the chiral condensates for u and d quarks, as a function of eB , for the QM model. The magnetic field splits the two quantities because of the different charge for the two quarks. The small oscillations, which are more evident for the case of the u -quark, are an artifact of the regularization scheme, and disappear if smoother regulators are used, see the discussion in [29]. In the regime of weak fields, our data are consistent with the scaling $\langle \bar{f}f \rangle \propto |eB|^2/M$ where M denotes some mass scale; in the strong field limit we find instead $\langle \bar{f}f \rangle \propto |eB|^{3/2}$. The behavior of the quark condensate as a function of magnetic field is in agreement with the magnetic catalysis scenario [27, 51].

In the lower panel of Fig. 1 we plot our data for the expectation value of the magnetic moment. Data correspond to the QM model (for the NJL model we obtain similar results). At weak fields, $\Sigma_f \propto |eB|$ as expected from Eq. (15). In the strong field limit, non-linearity arise because of the scaling of quark mass (or chiral con-

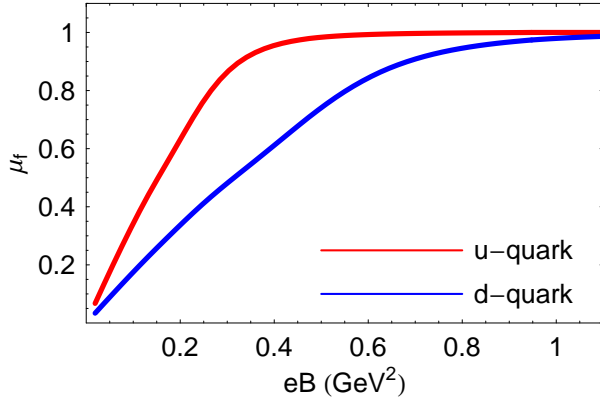


FIG. 2. Polarization of u -quarks (red) and d -quarks (blue) as a function of the magnetic field strength, for the QM model.

densate); we find $\Sigma_f \propto |eB|^{3/2}$ in this limit.

In Fig. 2 we plot our results for the polarization. Data are obtained by the previous ones, using the definition (3). At small fields, the polarization clearly grows linearly with the magnetic field. This is a natural consequence of the linear behavior of the magnetic moment as a function of eB for small fields, see Fig. 1. On the other hand, within the chiral models we measure a saturation of μ_f at large values of eB , to an asymptotic value $\mu_\infty = 1$. This conclusion remains unchanged if we consider the NJL model, and it is in agreement with the recent Lattice findings [41]. It should be noticed that, at least for the u -quark, saturation is achieved before the expected threshold for ρ -meson condensation [46–48]. Therefore, our expectation is that our result is stable also if vector meson condensation is considered.

The saturation to the asymptotic value $\mu_\infty = 1$ of polarization is naturally understood within the models we investigate, as a LLL dominance in the chiral condensate (i.e., full polarization). As a matter of fact, Σ_f and $\langle \bar{f}f \rangle$ turn to be proportional in the strong field limit, since only the LLL gives a contribution to the latter, compare Eq. (13) and (17) which imply

$$\mu_f = 1 - \frac{\langle \bar{f}f \rangle_{\text{HLL}}}{\langle \bar{f}f \rangle}, \quad (22)$$

where $\langle \bar{f}f \rangle_{\text{HLL}}$ corresponds to the higher Landau levels contribution to the chiral condensate. In the strong field limit $\langle \bar{f}f \rangle_{\text{HLL}} \rightarrow 0$ because of Eq. (12) which is a rough approximation to the QCD effective quark mass, as depicted in Eq. (14); hence, μ_f has to approach the asymptotic value $\mu_\infty = 1$. On the other hand, in the weak field limit $\langle \bar{f}f \rangle_{\text{HLL}} \rightarrow \langle \bar{f}f \rangle$ and the proportionality among Σ_f and $\langle \bar{f}f \rangle$ is lost.

In Ref. [41], data of polarization are fit by means of

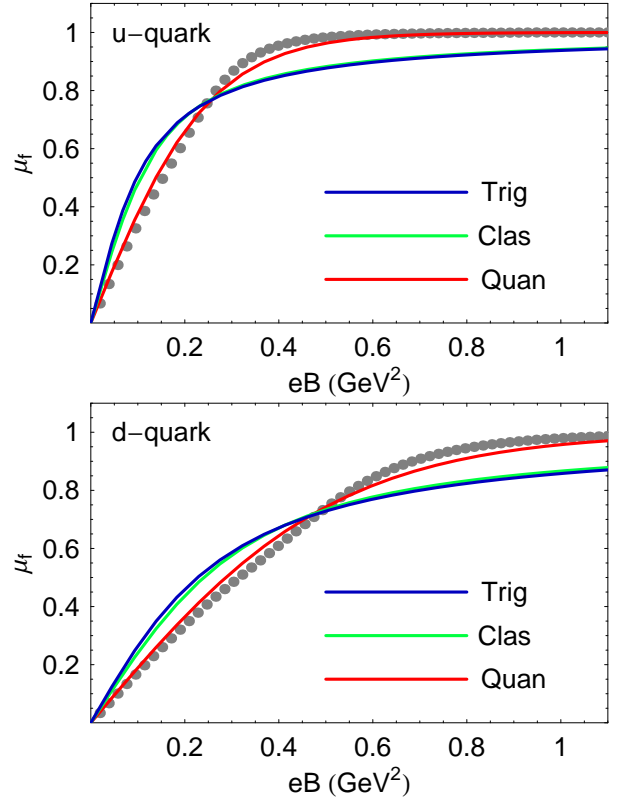


FIG. 3. *Upper panel.* Polarization data for u -quark (grey dots) and fitting curves. See the text for details. *Lower panel.* Polarization data and fitting functions for d -quark. Results correspond to the QM model.

three different functions, namely

$$\mu_f^{\text{clas}} = \mu_\infty \left| \coth \frac{3\chi Q_f eB}{\mu_\infty} - \frac{\mu_\infty}{3\chi Q_f eB} \right|, \quad (23)$$

$$\mu_f^{\text{quan}} = \mu_\infty \left| 2 \coth \frac{2\chi Q_f eB}{\mu_\infty} - \coth \frac{\chi Q_f eB}{\mu_\infty} \right|, \quad (24)$$

$$\mu_f^{\text{trig}} = \frac{2\mu_\infty}{\pi} \arctan \left| \frac{\pi\chi Q_f eB}{2\mu_\infty} \right|. \quad (25)$$

The three functions above share the behavior at the origin, $\mu_f \approx |\chi Q_f eB|$, and the asymptotic one, $\mu_f \approx \mu_\infty$. In [41] a two-parameter fit on χ and μ_∞ is performed; the model with the lowest chi-squared per degrees of freedom is represented by the trigonometric one, Eq. (25). Inspired by these results we have tried to fit our data using the same functions (23)–(25). In our model calculation, the asymptotic value $\mu_\infty = 1$ is achieved straightforwardly, therefore it is enough to perform a one-parameter fit leaving χ as a free parameter. The results of this procedure are collected in Fig. 3, where we plot our data of quark's polarization as a function of eB (gray dots) and the three fitting functions with $\mu_\infty = 1$. From Fig. 3 we read that both the trigonometric and the classic functions do not adapt well to our data (for the NJL model we obtain similar results). In particular, both of the afore-

mentioned functions overestimate χ , and reach slowly the asymptotic value. On the other hand, the quantum function in Eq. (24) offers a better description of our data in the whole range of eB examined here. We have checked that the value of χ obtained within this fit overestimates the value obtained by a weak-field linear fit only of the 10%, see below. Moreover, the fit functions smoothly follow the large eB data to the asymptotic value $\mu_f = 1$. We conclude that within our model, the quantum fitting function is a more faithful representation of data. The difference with Lattice data is probably due to the fact that the latter ones are obtained with quenched (hence, non-dynamical) fermions, while in our case dynamical fermions are considered. It will be interesting, therefore, to compare the model predictions with Lattice data obtained with other kinds of fermions in the near future.

Before going ahead, it is interesting that our data on polarization, and our interpretation of the saturation of the latter at large fields, gives a quantitative estimate of the goodness of the LLL approximation for the models at hand. In particular, at $eB_c \approx 0.6 \text{ GeV}^2$, which in turns is the estimated critical value for vector meson condensation [46, 48], the LLL almost dominates the chiral condensate of the u -quark; on the other hand, at this value of eB the LLL dominance has not yet been achieved for the d -quark condensate; but the higher Landau levels at this value of eB give a contribution almost to the 20% of the chiral condensate. This is an indirect check of the consistence of the LLL approximation used in [47], which in turn should be good within a 20% accuracy.

B. Magnetic susceptibility of the quark condensate

At small fields $\mu_f = |\chi Q_f eB|$ from Eq. (1). Hence, we use the data on polarization at small fields, to obtain the numerical value of the magnetic susceptibility of the chiral condensate. Our results are as follows:

$$\chi \approx -4.3 \text{ GeV}^{-2}, \quad \text{NJL} \quad (26)$$

$$\chi \approx -5.25 \text{ GeV}^{-2}, \quad \text{QM} \quad (27)$$

respectively for the NJL model and the QM model. To obtain the numerical values above we have used data for eB up to $5m_\pi^2 \approx 0.1 \text{ GeV}^2$, which are then fit using a linear law. Using the numerical values of the chiral condensate in the two models, we obtain

$$\chi \langle \bar{f}f \rangle \approx 69 \text{ MeV}, \quad \text{NJL} \quad (28)$$

$$\chi \langle \bar{f}f \rangle \approx 65 \text{ MeV}, \quad \text{QM} \quad (29)$$

The numerical values of χ that we obtain within the effective models are in fair agreement with recent results, see Table I. In our model calculations, the role of the renormalization scale is played approximately by the ultraviolet cutoff, that is Λ in Eq. (11), which is equal to 0.560 GeV in the QM model, and 0.627 GeV in the NJL model.

To facilitate the comparison with previous estimates, we review briefly the frameworks in which the results in

Table I are obtained. In [36] the following result is found, within OPE combined with Pion Dominance (we follow when possible the notation used in [41]):

$$\chi^{PD} = -c_\chi \frac{N_c}{8\pi^2 F_\pi^2}, \quad \text{Pion Dominance} \quad (30)$$

with $F_\pi = \sqrt{2}f_\pi = 130.7 \text{ MeV}$ and $c_\chi = 2$; the estimate of [36] is done at a renormalization point $M = 0.5 \text{ GeV}$. It is remarkable that Eq. (30) has been reproduced recently within AdS/QCD approach in [38]. Probably, this is the result more comparable to our estimate, because the reference scales in [36] and in this article are very close. Within our model calculations we find $c_\chi^{NJL} = 1.93$ and $c_\chi^{QM} = 2.36$. Using the numerical value of F_π and c_χ we get $\chi^{PD} = -4.45 \text{ GeV}^{-2}$, which agrees within 3% with our NJL model result, and within 18% with our QM model result.

In [37] the authors find $c_\chi = 2.15$ within hard-wall holographic approach, at the scale $M \ll 1 \text{ GeV}$. The results of [37] are thus in very good parametric agreement with [36]; on the other hand, the numerical value of F_π in the holographic model is smaller than the one used in [36], pushing the holographic prediction for χ to slightly higher values than in [36]. However, the scale at which the result of [37] is valid should be much smaller than $M = 1 \text{ GeV}$, thus some quantitative disagreement with [36] is expected. As the authors have explained, it might be possible to tune the parameters of the holographic model, mainly the chiral condensate, to reproduce the correct value of F_π ; their numerical tests suggest that by changing the ratio $\langle \bar{f}f \rangle / m_\rho$ of a factor of 8, then the numerical value of c_χ is influenced only by a 5%. It is therefore plausible that a best tuning makes the quantitative prediction of [37] much closer to the estimate of [36].

In [39] an estimate of χ within the instanton vacuum model has been performed beyond the chiral limit, both for light and for strange quarks (the result quoted in Table I corresponds to the light quarks; for the strange quark, $\chi_s / \chi_{u,d} \approx 0.15$ is found). Taking into account the numerical value of the chiral condensate in the instanton vacuum, the numerical estimate of [39] leads to $\chi = -2.5 \pm 0.15 \text{ GeV}^{-2}$ at the scale $M = 1 \text{ GeV}$. An analytic estimate within a similar framework has been obtained in [40], in which the zero-mode of the Dirac operator in the background of a $SU(2)$ instanton is used to compute the relevant expectation values. The result of [31] gives $\chi = -3.52 \text{ GeV}^{-2}$ at $M \approx 1 \text{ GeV}$.

In [41] the result $\chi = -1.547 \text{ GeV}^{-2}$ is achieved within a two-color simulation with quenched fermions. It is interesting that in [41] the same quantity has been computed also at finite temperature in the confinement phase, at $T = 0.82T_c$, and the result seems to be independent on temperature. The reference scale of [41], determined by the inverse lattice spacing, is $M \approx 2 \text{ GeV}$. Therefore the lattice results are not quantitatively comparable with our model calculation. However, they share

an important feature with the results presented here, namely the saturation of the polarization at large values of the magnetic field. Finally, estimates of the magnetic susceptibility of the chiral condensate by means of several QCD sum rules there exist [31–35]. The results are collected in Table I.

IV. RENORMALIZED QM MODEL

In this Section, we make semi-analytic estimates of the polarization and the magnetic susceptibility of the quark condensate, as well as for the chiral condensate in magnetic background, within the renormalized QM model. This is done with the scope to compare the predictions of the renormalized model with those of the effective models, in which an ultraviolet cutoff is introduced to mimic the QCD effective quark mass.

In the renormalized model, we allow the effective quark mass to be a constant in the whole range of momenta, which is different from what happens in QCD [45]. Thus, the higher Landau levels give a finite contribution to the vacuum chiral condensate even at very strong fields. This is easy to understand: the ultraviolet cutoff, Λ , in the renormalized model can be taken larger than any other mass scale, in particular $\Lambda \gg |eB|^{1/2}$; as a consequence, the condition $p_3^2 + 2n|eB| < \Lambda^2$ is satisfied taking into account many Landau levels even at very large eB . The contribution of the higher Landau levels, once renormalized, appears in the physical quantities to which we are interested here, in particular in the chiral condensate.

Since the computation is a little bit lengthy, it is useful to anticipate its several steps: firstly we perform regularization, and then renormalization, of the QEP at zero magnetic field (the corrections due to the magnetic field turn out to be free of ultraviolet divergences). Secondly, we solve analytically the gap equation for the σ condensate in the limit of weak fields, and semi-analytically in the opposite limit. The field-induced corrections to the QEP and to the solution of the gap equation are divergence-free in agreement with [27], and are therefore independent on the renormalization scheme adopted. Then, we compute the renormalized and self-consistent values of the chiral condensate and of the magnetic moment, as a function of eB , using the results for the gap equation. Within this theoretical framework, it is much more convenient to compute $\langle \bar{f}f \rangle$ and Σ_f by taking derivatives of the renormalized potential; in fact, the computation of the traces of the propagator in the renormalized model is much more involved if compared to the situation of the non-renormalized models, since in the former a non-perturbative (and non-trivial) renormalization procedure of composite local operators is required [54]. Finally, we estimate χ , as well as the behavior of the polarization as a function of eB .

A. Renormalization of the QEP

To begin with, we need to regularize the one-loop fermion contribution in Eq. (9) namely

$$V_{1\text{-loop}}^{\text{fermion}} = -N_c \sum_f \frac{|Q_f eB|}{2\pi} \times \sum_{n=0}^{\infty} \beta_n \int_{-\infty}^{+\infty} \frac{dk}{2\pi} (k^2 + 2n|Q_f eB| + m_q^2)^{1/2}. \quad (31)$$

To this end, we define the function, $\mathcal{V}(s)$, of a complex variable, s , as

$$\mathcal{V}(s) = -N_c \sum_f \frac{|Q_f eB|}{2\pi} \times \sum_{n=0}^{\infty} \beta_n \int_{-\infty}^{+\infty} \frac{dk}{2\pi} (k^2 + 2n|Q_f eB| + m_q^2)^{\frac{1-s}{2}}. \quad (32)$$

The function $\mathcal{V}(s)$ can be analytically continued to $s = 0$. We define then $V_{1\text{-loop}}^{\text{fermion}} = \lim_{s \rightarrow 0^+} \mathcal{V}(s)$. After elementary integration over k , summation over n and taking the limit $s \rightarrow 0^+$, we obtain the result

$$V_{1\text{-loop}}^{\text{fermion}} = N_c \sum_f \frac{(Q_f eB)^2}{4\pi^2} \left(\frac{2}{s} - \log(2|Q_f eB|) + a \right) B_2(q) - N_c \sum_f \frac{(Q_f eB)^2}{2\pi^2} \zeta'(-1, q) - N_c \sum_f \frac{|Q_f eB| m_q^2}{8\pi^2} \left(\frac{2}{s} - \log(m_q^2) + a \right), \quad (33)$$

where we have subtracted terms which do not depend explicitly on the condensate. In the above equation, $\zeta(t, q)$ is the Hurwitz zeta function; for $\text{Re}(t) > 1$ and $\text{Re}(q) > 0$, it is defined by the series $\zeta(t, q) = \sum_{n=0}^{\infty} (n+q)^{-t}$; the series can be analytically continued to a meromorphic function defined in the complex plane $t \neq 1$. Moreover we have defined $q = (m_q^2 + 2|Q_f eB|)/2|Q_f eB|$; furthermore, $a = 1 - \gamma_E - \psi(-1/2)$, where γ_E is the Euler-Mascheroni number and ψ is the digamma function. The derivative $\zeta'(-1, q) = d\zeta(t, q)/dt$ is understood to be computed at $t = -1$.

The first two addenda in Eq. (33) arise from the higher Landau levels; on the other hand, the last addendum is the contribution of the LLL. The function B_2 is the second Bernoulli polynomial; using its explicit form, it is easy to show that the divergence in the LLL term in Eq. (33) is canceled by the analogous divergence in the first addendum of the same equation. It is interesting that the LLL contribution, which is in principle divergent, combines with a part of the contribution of the higher Landau levels, leading to a finite result. This can be interpreted as a renormalization of the LLL contribution. On the other hand, the remaining part arising

Method	χ (GeV $^{-2}$)	Ren. Point (GeV)	Ref.
Sum rules	-8.6 ± 0.24	1	[31]
Sum rules	-5.7	0.5	[32]
Sum rules	-4.4 ± 0.4	1	[33]
Sum rules	-3.15 ± 0.3	1	[34]
Sum rules	-2.85 ± 0.5	1	[35]
OPE + Pion Dominance	$-N_c/(4\pi^2 F_\pi^2)$	0.5	[36]
Holography	$-1.075 N_c/(4\pi^2 F_\pi^2)$	$\ll 1$	[37]
Holography	$-N_c/(4\pi^2 F_\pi^2)$	$\ll 1$	[38]
Instanton vacuum	-2.5 ± 0.15	1	[39]
Zero mode of Dirac Operator	-3.52	1	[40]
Lattice	$-1.547(3)$	2	[41]
NJL model	-4.3	0.63	This work
QM model	-5.25	0.56	This work

TABLE I. Magnetic susceptibility of the quark condensate obtained within several theoretical approaches. In the table, $F_\pi = 130.7$ MeV. See the text for more details.

from the higher Landau levels is still divergent; this divergence survives in the $\mathbf{B} \rightarrow 0$ limit, and is due to the usual divergence of the vacuum contribution. We then have

$$\begin{aligned}
V_{1\text{-loop}}^{\text{fermion}} = & N_c \sum_f \frac{m_q^4}{16\pi^2} \left(\frac{2}{s} - \log(2|Q_f e B|) + a \right) \\
& + N_c \sum_f \frac{|Q_f e B| m_q^2}{8\pi^2} \log \frac{m_q^2}{2|Q_f e B|} \\
& - N_c \sum_f \frac{(Q_f e B)^2}{2\pi^2} \zeta'(-1, q) . \quad (34)
\end{aligned}$$

The divergence of the vacuum energy is made explicit in the expression in the square brackets in Eq. (34). The mathematical structure of the divergence, namely a pole in $s = 0$ and a logarithm with a dimensional argument, is similar to that obtained within the dimensional regularization scheme. The scale of the logarithm is hidden in the $1/s$ term, and appears explicitly when the divergence is subtracted. Such a divergence affects only the $\mathbf{B} = 0$ effective potential; the corrections due to the magnetic field are either finite or independent on the condensate. As a matter of fact, in the zero magnetic field limit $q \rightarrow \infty$, the fermion bubble becomes

$$N_c N_f \frac{m_q^4}{16\pi^2} \left(\frac{2}{s} - \log m_q^2 + a + \frac{1}{2} \right) \equiv V_0 , \quad (35)$$

where we have used the relation

$$\zeta'(-1, q) \approx \left(\frac{1}{12} - \frac{q^2}{4} \right) + \log(q) \frac{B_2(q)}{2} , \quad (36)$$

with B_2 corresponding to the second Bernoulli polynomial. Using Eqs. (35) and (34) we notice that the pole

$2/s$ is cancelled in the difference $V_1 \equiv V_{1\text{-loop}}^{\text{fermion}} - V_0$,

$$\begin{aligned}
V_1 = & -N_c \sum_f \left(\frac{m_q^4}{16\pi^2} + \frac{|Q_f e B| m_q^2}{8\pi^2} \right) \log \frac{2|Q_f e B|}{m_q^2} \\
& - N_c \sum_f \frac{|Q_f e B|^2}{2\pi^2} \zeta'(-1, q) - N_c N_f \frac{m_q^4}{32\pi^2} . \quad (37)
\end{aligned}$$

To remove the divergence of the vacuum term, we follow Ref. [27] and adopt the renormalization conditions that at zero magnetic field, the quantum corrections do not shift the classical expectation value of the σ field in the vacuum, $\langle \sigma \rangle = f_\pi$, as well as the classical value m_σ^2 . To fulfill these conditions, two counterterms have to be added to the effective potential, $V^{\text{c.t.}} = \delta\lambda \times \sigma^4/4 + \delta v \times \sigma^2/2$. This amounts to require

$$\left. \frac{\partial(V_0 + V^{\text{c.t.}})}{\partial\sigma} \right|_{\sigma=f_\pi} = \left. \frac{\partial^2(V_0 + V^{\text{c.t.}})}{\partial\sigma^2} \right|_{\sigma=f_\pi} = 0 . \quad (38)$$

Taking into account the one-loop divergent contribution and the condition (38), we can write the renormalized potential at zero field as

$$V = \frac{\tilde{\lambda}}{4} (\sigma^2 - \tilde{v}^2)^2 - h\sigma - \frac{N_c N_f m_q^4}{16\pi^2} \log \frac{m_q^2}{g^2 f_\pi^2} , \quad (39)$$

where $\tilde{\lambda}$ and \tilde{v} are the renormalized parameters, whose expression is not needed here. Equation (39) is in agreement with the textbook result for the one-loop effective potential of a linear sigma model coupled to fermions by means of a Yuwaka-type interaction [52]. This is a consistency check of our regularization and renormalization procedures.

B. Approximate solutions of the gap equation

Weak fields. We now restore the magnetic field, and

firstly take the weak field limit. In this context, small field means $eB \ll m_q^2$. Using again Eq. (36) we notice that the derivative of the ζ -function cancels the other addenda in Eq. (37), and the remaining contribution is

$$\begin{aligned} V_1 &\approx -N_c \sum_f \frac{(Q_f eB)^2}{24\pi^2} \log \frac{m_q^2}{2|Q_f eB|} \\ &= -N_c \sum_f \frac{(Q_f eB)^2}{24\pi^2} \log \frac{m_q^2}{\mu^2}, \end{aligned} \quad (40)$$

which is in agreement with the result of [27]. In the above equation we have followed the notation of [43] introducing an infrared scale μ , isolating and then subtracting the term which does not depend on the condensate. The scale μ is arbitrary, and we cannot determine it from first principles; on the other hand, it is irrelevant for the determination of the σ -condensate. We expect $\mu \approx f_\pi$ since this is the typical scale of chiral symmetry breaking in the model for the σ field. The correction (40) lowers the effective potential of the broken phase, thus favoring the spontaneous breaking of chiral symmetry. The result in Eq. (40) is UV divergence-free as anticipated; thus, it is independent on the particular procedure used to regularize the QEP.

In this limit, it is easy to obtain analytically the behavior of the constituent quark mass as a function of eB . As a matter of fact, we can expand the derivative of the QEP with respect to σ , around the solution at $B = 0$, writing $\langle \sigma \rangle = f_\pi + \delta\sigma$. Then, a straightforward evaluation leads to

$$m_q = g f_\pi \left(1 + \frac{5}{9} \frac{N_c}{12\pi^2 f_\pi^2 m_\sigma^2} (eB)^2 \right). \quad (41)$$

As anticipated, the scale μ is absent in the solution of the gap equation.

Strong fields. In the limit $eB \gg m_q^2$, we can find an asymptotic representation of V_1 by using the expansion $\zeta'(-1, q) = c_0 + c_1(q-1)$ valid for $q \approx 1$, with $c_0 = -0.17$ and $c_1 = -0.42$. Then we find

$$\begin{aligned} V_1 &\approx -N_c \sum_f \frac{m_q^2}{8\pi^2} \left(\frac{m_q^2}{2} + |Q_f eB| \right) \log \frac{2|Q_f eB|}{m_q^2} \\ &\quad - N_c \sum_f \frac{|Q_f eB| m_q^2}{2\pi^2} c_1, \end{aligned} \quad (42)$$

where we have subtracted condensate-independent terms.

In the strong field limit it is not easy to find analytically an asymptotic representation for the sigma condensate as a function of eB ; therefore we solve the gap equation numerically, and then fit data with a convenient analytic form as follows:

$$m_q = b|eB|^{1/2} + \frac{c f_\pi^3}{|eB|}, \quad (43)$$

where $b = 0.32$ and $c = 32.78$. At large fields the quark mass grows as $|eB|^{1/2}$ as expected by dimensional analysis; this is a check of the equations that we use.

C. Evaluation of chiral condensate and magnetic moment

Chiral condensate. To compute the chiral condensate we follow a standard procedure: we introduce source term for $\bar{f}f$, namely a bare quark mass m_f , then take derivative of the effective potential with respect to m_f evaluated at $m_f = 0$. This amounts to derive only $V_{1-\text{loop}}^{\text{fermion}}$, since both the classic potential and counterterms do not have a dependence on m_f . According to Eq. (37) we find

$$\langle \bar{f}f \rangle = \left. \frac{\partial V_0}{\partial m_f} \right|_{m_f=0} + \left. \frac{\partial V_1}{\partial m_f} \right|_{m_f=0}. \quad (44)$$

The first and second addenda on the r.h.s. of Eq. (44) represent the vacuum and the field-induced contributions to the chiral condensate respectively. The vacuum contribution is divergent, and can be renormalized according to the procedure of renormalization of composite local operators [54]. It is not necessary to perform this procedure here, because the numerical value of the vacuum condensate is not necessary in our discussion¹. Therefore, it is enough to compute only the contribution at $B \neq 0$ arising from V_1 , which is finite.

In particular, for the weak field case we obtain

$$\langle \bar{f}f \rangle = \langle \bar{f}f \rangle_0 - \frac{N_c}{12\pi^2} \frac{|Q_f eB|^2}{m_q}. \quad (45)$$

On the other hand, in the strong field limit we have

$$\langle \bar{f}f \rangle = -\frac{N_c m_q}{4\pi^2} (|Q_f eB| + m_q^2) \log \frac{2|Q_f eB|}{m_q^2}. \quad (46)$$

Using Equations (41) and (43), we show that the chiral condensate scales as $a + b(eB)^2$ for small fields, and as $|eB|^{3/2}$ for large fields.

Magnetic moment. Next we turn to the computation of the expectation value of the magnetic moment. The expression in terms of Landau levels is given by Eq. (17), which clearly shows that this quantity has a log-type divergence. In order to avoid a complicated renormalization procedure of a local composite operator, we notice that it is enough to take the minus derivative of V_1 with respect to B to get magnetization, \mathcal{M} [43], then multiply by $2m/Q_f$ to get the magnetic moment. This procedure is very cheap, since the B -dependent contributions to the effective potential are finite, and the resulting expectation value will turn out to be finite as well (that is, already renormalized).

¹ In principle, in the renormalization program of the composite operator $\langle \bar{q}q \rangle$ one can impose, as a renormalization condition, that the chiral condensate in the vacuum is consistent with the results of [49] at the renormalization point $M = 1$ GeV.

In the case of weak fields, from Eq. (40) we find

$$\Sigma_f = N_c \frac{Q_f |eB| m_q}{6\pi^2} \log \frac{m_q^2}{\mu^2}. \quad (47)$$

On the other hand, in the strong field limit we get from Eq. (42)

$$\Sigma_f = N_c \frac{m_q^3}{4\pi^2} \log \frac{2|Q_f eB|}{m_q^2}. \quad (48)$$

The above result is in parametric agreement with the estimate of magnetization in [43]. In fact, $m_q^2 \approx |eB|$ in the strong field limit, which leads to a magnetization $\mathcal{M} \approx B \log B$.

Using the expansions for the sigma condensate at small and large values of the magnetic field strength, we argue that $\Sigma_f \approx |eB|$ in a weak field, and $\Sigma_f \approx |eB|^{3/2}$ in a strong field.

D. Computation of chiral magnetization and polarization

We can now estimate the magnetic susceptibility of the quark condensate and the polarization as a function of eB . For the former, we need to know the behavior of the magnetic moment for weak fields. From Eq. (47) and from the definition (1) we read

$$\chi \langle \bar{f} f \rangle = \frac{N_c m_q}{6\pi^2} \log \frac{m_q^2}{\mu^2} \equiv f(\mu). \quad (49)$$

The presence of the infrared scale μ makes the numerical estimate of χ uncertain; however, taking for it a value $\mu \approx f_\pi$, which is the typical scale of chiral symmetry breaking, we have $\chi \langle \bar{f} f \rangle \approx 44$ MeV, which is in agreement with the expected value, see Eq. (2). In Fig. 4 we plot $f(\mu)$ as a function of μ . The interval on the μ -axis delimited by the green and the blue vertical lines is the range in which we obtain a value of χ which is consistent with phenomenology.

Next we turn to the polarization. For weak fields we find trivially a linear dependence of μ_f on $|Q_f eB|$, with slope given by the absolute value of χ in Eq. (49). On the other hand, in the strong field limit we find, according to Eq. (48),

$$\mu_f \approx \frac{m_q^2}{m_q^2 + |Q_f eB|} \approx 1 - \frac{|Q_f|}{b + |Q_f|}, \quad (50)$$

where we have used Eq. (43). This result shows that the polarization saturates at large values of eB , but the asymptotic value depends on the flavor charge.

It is interesting to compare the result of the renormalized model with that of the effective models considered in the previous Section. In the former, the asymptotic value of μ_f is flavor-dependent; in the latter, $\mu_f \rightarrow 1$ independently on the value of the electric charge. Our

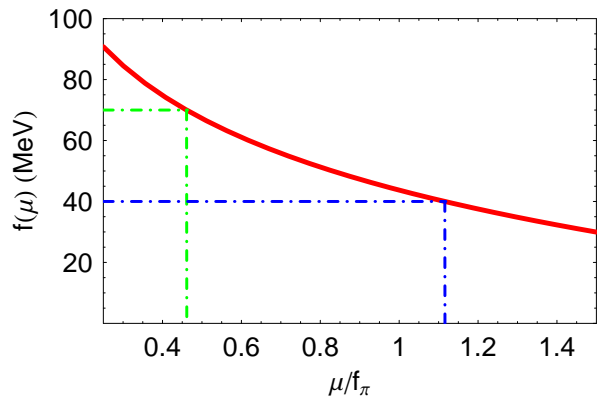


FIG. 4. Magnetic susceptibility of the quark condensate multiplied by the chiral condensate, in MeV, as a function of the infrared scale μ , as given by Eq. (49). The interval on the μ -axis delimited by the green and the blue vertical lines is the range in which we obtain a value of χ which is consistent with phenomenology.

interpretation of this difference is as follows: comparing Eq. (50) with the general model expectation, Eq. (22), we recognize in the factor $|Q_f|/(b + |Q_f|)$ the contribution of the higher Landau levels at zero temperature, which turns out to be finite and non-zero after the renormalization procedure. This contribution is then transmitted to the physical quantities that we have computed. The trace of the higher Landau levels is implicit in the solution of the gap equation in the strong field limit, namely the factor b in Eq. (43), and explicit in the additional $|Q_f|$ dependence in Eq. (50). A posteriori, this conclusion seems quite natural, because in the renormalization procedure we assume that the effective quark mass is independent on quark momentum, thus there is no cut of the large momenta in the gap equation (and in the equation for polarization as well). In the effective models considered in the first part of this article, on the other hand, the cutoff procedure is equivalent to have a momentum-dependent effective quark mass, $m_q = g\sigma\Theta(\Lambda^2 - p_3^2 - 2n|Q_f eB|)$, which naturally cuts off higher Landau levels when $eB \gg \Lambda^2$. At the end of the days, the expulsion of the higher Landau levels from the chiral condensate makes $\mu_f \rightarrow 1$ in the strong field limit. Our expectation is that if we allow the quark mass to run with momentum and decay rapidly at large momenta, mimicking the effective quark mass of QCD, higher Landau levels would be suppressed in the strong field limit, and the result (50) would tend to the result in Fig. 2.

V. CONCLUSIONS

In this article, we have computed the magnetic susceptibility of the quark condensate, χ , and the polarization, μ_f , in a background of a magnetic field, \mathbf{B} , by means of

two chiral models of QCD: the quark-meson model and the Nambu-Jona-Lasinio model. The knowledge of these quantities is relevant both theoretically and phenomenologically. Indeed, the magnetic susceptibility of the quark condensate might lead, in the photoproduction of lepton pairs, to an interference between the Drell-Yan process and the photon-quark coupling, the latter induced by the chiral-odd distribution amplitude of the quark [42]. The two models are widely used to study the phase diagram of QCD in several regimes; it has been proved in different contexts, that they offer a good theoretical tool to compute low-energy QCD properties. It is thus interesting to compute, within these models, quantities which characterize the QCD vacuum in a magnetic background, and compare the results with those obtained within different theoretical frameworks, both analytically and numerically.

In the first part of this article, we have reported our results about χ and μ_f obtained within a numerical self-consistent solution of the model, in the one-loop approximation. Our results on χ are summarized in Table I, and are in fair agreement with previous estimates. Besides, our data on polarization are collected in Fig. 3. For the latter, we obtain a saturation to the asymptotic value $\mu_\infty = 1$ at large values of eB , which is understood as a lowest Landau level dominance in the quark condensate. This is in agreement with recent results obtained within Lattice QCD simulations with two colors and quenched fermions [41].

In the second part of the article, we have estimated χ and μ_f within a renormalized version of the QM model. The numerical value of χ in this case is quite uncertain because of the presence, in the final result, of an unknown infrared scale μ . However, as shown in Fig. 4, taking for μ a numerical value around f_π , which is the typical scale of chiral symmetry breaking in this model, we obtain a value of χ which is consistent with phenomenology.

Within the renormalized model we find a saturation of μ_f at large B , in qualitative agreement with our findings within the effective models in Section III and quenched

QCD [41]. In the renormalized model, the asymptotic value of μ_f is flavor-dependent; in the effective models and quenched QCD, $\mu_f \rightarrow 1$ independently on the value of the electric charge. We attribute this difference to the presence, in the theory, of the renormalized contribution of the higher Landau levels: in the renormalized model, the higher Landau levels give a finite contribution to the chiral condensate at zero temperature, even in the case of very strong fields. After renormalization of the QEP, this contribution is finite and non-zero, and is transmitted to the physical quantities that we have computed.

The results we obtained are quite encouraging, and suggest that a systematic study of external field induced condensates at zero, as well as finite, temperature within chiral models is worth to be done. As a natural continuation of this study, it would be interesting to add the strange quark, following the work [39]. Moreover, Lattice simulations have shown that χ is almost insensitive to the temperature, at least in the confinement phase [41]. This result is achieved with quenched fermions. On the other hand, the chiral model handle with dynamical fermions; it would be therefore of interest to address the question of the behavior of χ as a function of temperature using chiral models. Furthermore, it has been shown [53] that local fluctuations of topological charge induce a quark electric dipole moment along the direction of a strong magnetic field. This problem can be studied easily within the chiral models, introducing a pseudo-chemical potential μ_5 conjugated to chirality imbalance as already done in [24, 30].

Acknowledgements. We acknowledge M. Chernodub, T. Cohen, A. Flachi, R. Gatto, A. Ohnishi for several discussions and correspondence. Moreover, we thank H. Suganuma for valuable and numerous discussions on the renormalization of the quark-meson model and for a careful reading of the manuscript. The Laboratoire de Mathematique et Physique Theorique of Tours University, as well as the Physics Department of Jyväskylä University, where part of this work was completed, are acknowledged for the kind hospitality. The work of M. R. is supported by JSPS under contract number P09028.

-
- [1] P. de Forcrand and O. Philipsen, JHEP **0701**, 077 (2007); JHEP **0811**, 012 (2008); PoS **LATTICE2008**, 208 (2008).
 - [2] Y. Aoki *et al.*, Nature **443**, 675 (2006); Y. Aoki, S. Borsanyi, S. Durr, Z. Fodor, S. D. Katz, S. Krieg and K. K. Szabo, JHEP **0906**, 088 (2009); S. Borsanyi *et al.*, S. Borsanyi *et al.*, JHEP **1009** (2010) 073;
 - [3] A. Bazavov *et al.*, Phys. Rev. D **80**, 014504 (2009).
 - [4] M. Cheng *et al.*, Phys. Rev. D **81**, 054510 (2010).
 - [5] F. Karsch, E. Laermann and A. Peikert, Nucl. Phys. B **605**, 579 (2001); F. Karsch, Lect. Notes Phys. **583**, 209 (2002); O. Kaczmarek and F. Zantow, Phys. Rev. D **71**, 114510 (2005).
 - [6] C. S. Fischer, Phys. Rev. Lett. **103**, 052003 (2009); C. S. Fischer and J. A. Mueller, Phys. Rev. D **80**, 074029 (2009); C. S. Fischer, A. Maas and J. A. Muller, Eur. Phys. J. C **68**, 165 (2010). A. C. Aguilar and J. Papavassiliou, arXiv:1010.5815 [hep-ph]; C. Feuchter and H. Reinhardt, Phys. Rev. D **70**, 105021 (2004); Phys. Rev. D **71**, 105002 (2005). M. Leder, J. M. Pawłowski, H. Reinhardt and A. Weber, arXiv:1006.5710 [hep-th]; J. Braun, Eur. Phys. J. C **64**, 459 (2009); J. Braun, L. M. Haas, F. Marhauser and J. M. Pawłowski, arXiv:0908.0008 [hep-ph]; J. Braun and A. Janot, arXiv:1102.4841 [hep-ph].
 - [7] M. Frasca, Phys. Lett. B **670**, 73 (2008); Mod. Phys. Lett. A **24** (2009) 2425; arXiv:1007.4479 [hep-ph].
 - [8] M. A. Shifman, A. I. Vainshtein and V. I. Zakharov, Nucl. Phys. B **147**, 385 (1979); Nucl. Phys. B **147**, 448 (1979).
 - [9] Y. Nambu and G. Jona-Lasinio, Phys. Rev. **122**, 345

- (1961); Y. Nambu and G. Jona-Lasinio, Phys. Rev. **124**, 246 (1961).
- [10] U. Vogl and W. Weise, Prog. Part. Nucl. Phys. **27**, 195 (1991); S. P. Klevansky, Rev. Mod. Phys. **64**, 649 (1992); T. Hatsuda and T. Kunihiro, Phys. Rept. **247**, 221 (1994); M. Buballa, Phys. Rept. **407**, 205 (2005).
- [11] K. I. Kondo, Phys. Rev. D **82**, 065024 (2010).
- [12] M. Frasca, Nucl. Phys. Proc. Suppl. **207-208**, 196 (2010); Int. J. Mod. Phys. E **18**, 693 (2009).
- [13] J. L. Gervais and B. W. Lee, Nucl. Phys. B **12**, 627 (1969).
- [14] A. L. Mota, M. C. Nemes, B. Hiller and H. Walliser, Nucl. Phys. A **652**, 73 (1999).
- [15] S. Weinberg, Phys. Rev. D **56**, 2303 (1997).
- [16] K. G. Wilson, Phys. Rev. D **7**, 2911 (1973); T. Eguchi, Phys. Rev. D **17**, 611 (1978); S. Kim, A. Kocic and J. B. Kogut, Nucl. Phys. B **429**, 407 (1994).
- [17] S. Roessner, C. Ratti and W. Weise, Phys. Rev. D **75**, 034007 (2007); C. Sasaki, B. Friman and K. Redlich, Phys. Rev. D **75**, 074013 (2007); S. K. Ghosh, T. K. Mukherjee, M. G. Mustafa and R. Ray, Phys. Rev. D **77**, 094024 (2008); A. Bhattacharyya, P. Deb, S. K. Ghosh and R. Ray, Phys. Rev. D **82**, 014021 (2010).
- [18] K. Fukushima, Phys. Rev. D **77**, 114028 (2008) [Erratum-ibid. D **78**, 039902 (2008)]; M. Ciminale, R. Gatto, N. D. Ippolito, G. Nardulli and M. Ruggieri, Phys. Rev. D **77**, 054023 (2008); W. j. Fu, Z. Zhang and Y. x. Liu, Phys. Rev. D **77**, 014006 (2008); T. Hell, S. Rossner, M. Cristoforetti and W. Weise, Phys. Rev. D **81**, 074034 (2010).
- [19] H. Abuki, R. Anglani, R. Gatto, G. Nardulli and M. Ruggieri, Phys. Rev. D **78**, 034034 (2008).
- [20] K. Kashiwa, H. Kouno, M. Matsuzaki and M. Yahiro, Phys. Lett. B **662**, 26 (2008); Y. Sakai, T. Sasaki, H. Kouno and M. Yahiro, Phys. Rev. D **82**, 076003 (2010).
- [21] T. K. Herbst, J. M. Pawłowski and B. J. Schaefer, arXiv:1008.0081 [hep-ph].
- [22] V. Skokov, B. Friman, E. Nakano, K. Redlich and B. J. Schaefer, Phys. Rev. D **82**, 034029 (2010).
- [23] T. Kahara and K. Tuominen, Phys. Rev. D **78**, 034015 (2008); Phys. Rev. D **80**, 114022 (2009); arXiv:1006.3931 [hep-ph].
- [24] K. Fukushima, M. Ruggieri and R. Gatto, Phys. Rev. D **81**, 114031 (2010).
- [25] A. J. Mizher, M. N. Chernodub and E. S. Fraga, Phys. Rev. D **82**, 105016 (2010).
- [26] R. Gatto and M. Ruggieri, Phys. Rev. D **83**, 034016 (2011); Phys. Rev. D **82**, 054027 (2010).
- [27] H. Suganuma and T. Tatsumi, Annals Phys. **208**, 470 (1991).
- [28] E. S. Fraga and A. J. Mizher, Phys. Rev. D **78**, 025016 (2008).
- [29] L. Campanelli and M. Ruggieri, Phys. Rev. D **80**, 034014 (2009).
- [30] M. N. Chernodub and A. S. Nedelin, arXiv:1102.0188 [hep-ph].
- [31] B. L. Ioffe and A. V. Smilga, Nucl. Phys. B **232**, 109 (1984).
- [32] V. M. Belyaev and Y. I. Kogan, Yad. Fiz. **40**, 1035 (1984).
- [33] I. I. Balitsky, A. V. Kolesnichenko and A. V. Yung, Sov. J. Nucl. Phys. **41**, 178 (1985) [Yad. Fiz. **41**, 282 (1985)].
- [34] P. Ball, V. M. Braun and N. Kivel, Nucl. Phys. B **649**, 263 (2003).
- [35] J. Rohrwild, JHEP **0709**, 073 (2007).
- [36] A. Vainshtein, Phys. Lett. B **569**, 187 (2003).
- [37] A. Gorsky and A. Krikun, Phys. Rev. D **79**, 086015 (2009).
- [38] D. T. Son and N. Yamamoto, arXiv:1010.0718 [hep-ph].
- [39] H. C. Kim, M. Musakhanov and M. Siddikov, Phys. Lett. B **608**, 95 (2005).
- [40] B. L. Ioffe, Phys. Lett. B **678**, 512 (2009).
- [41] P. V. Buividovich, M. N. Chernodub, E. V. Luschevskaya and M. I. Polikarpov, Nucl. Phys. B **826**, 313 (2010).
- [42] B. Pire and L. Szymanowski, Phys. Rev. Lett. **103**, 072002 (2009).
- [43] T. D. Cohen and E. S. Werbos, Phys. Rev. C **80**, 015203 (2009).
- [44] K. Langfeld, C. Kettner and H. Reinhardt, Nucl. Phys. A **608**, 331 (1996).
- [45] H. D. Politzer, Nucl. Phys. B **117**, 397 (1976); Phys. Lett. B **116**, 171 (1982).
- [46] M. N. Chernodub, Phys. Rev. D **82**, 085011 (2010).
- [47] M. N. Chernodub, arXiv:1101.0117 [hep-ph].
- [48] N. Callebaut, D. Dudal and H. Verschelde, arXiv:1102.3103 [hep-ph].
- [49] H. G. Dosch and S. Narison, Phys. Lett. B **417**, 173 (1998); S. Narison, Phys. Rev. D **74**, 034013 (2006).
- [50] V. I. Ritus, Annals Phys. **69**, 555 (1972); C. N. Leung and S. Y. Wang, Nucl. Phys. B **747**, 266 (2006).
- [51] S. P. Klevansky and R. H. Lemmer, Phys. Rev. D **39**, 3478 (1989); I. A. Shushpanov and A. V. Smilga, Phys. Lett. B **402**, 351 (1997); D. N. Kabat, K. M. Lee and E. J. Weinberg, Phys. Rev. D **66**, 014004 (2002); T. Inagaki, D. Kimura and T. Murata, Prog. Theor. Phys. **111**, 371 (2004); T. D. Cohen, D. A. McGady and E. S. Werbos, Phys. Rev. C **76**, 055201 (2007); V. P. Gusynin, V. A. Miransky and I. A. Shovkovy, Nucl. Phys. B **462**, 249 (1996); Nucl. Phys. B **563**, 361 (1999); G. W. Semenoff, I. A. Shovkovy and L. C. R. Wijewardhana, Phys. Rev. D **60**, 105024 (1999); V. A. Miransky and I. A. Shovkovy, Phys. Rev. D **66**, 045006 (2002); K. G. Klimenko, Theor. Math. Phys. **89**, 1161 (1992) [Teor. Mat. Fiz. **89**, 211 (1991)]; K. G. Klimenko, Z. Phys. C **54**, 323 (1992); K. G. Klimenko, Theor. Math. Phys. **90**, 1 (1992) [Teor. Mat. Fiz. **90**, 3 (1992)]; B. Hiller, A. A. Osipov, A. H. Blin and J. da Providencia, SIGMA **4**, 024 (2008); A. Goyal and M. Dahiya, Phys. Rev. D **62**, 025022 (2000).
- [52] S. Weinberg, *The Quantum Theory of Fields: Modern Applications*, Cambridge University Press, ISBN 978-0-521-67054-8.
- [53] P. V. Buividovich, M. N. Chernodub, E. V. Luschevskaya and M. I. Polikarpov, Phys. Rev. D **81**, 036007 (2010).
- [54] J. C. Collins, *Renormalization. An Introduction To Renormalization, The Renormalization Group, And The Operator Product Expansion*, Cambridge, UK: Univ. Pr. (1984).